Electronic Supplementary Material (ESI) for Nanoscale Advances.

Hydrothermal Synthesis of Carbon Nanodots from Bovine Gelatin and PHM3 Microalgae Strain for Anticancer and Bioimaging Applications

Supplementary Material

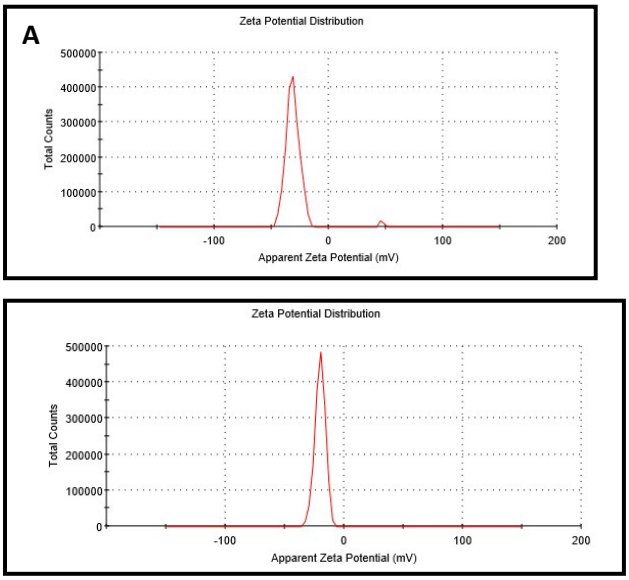

Figure S1 (A) showing zeta potential results of CG (bovine gelatin) nanodots (B) showing zeta potential of CA (algae) nanodots.

		Mean (mV)	Area (%)	St Dev (mV)
Z-Potential (mV): -30.3	Peak 1	-30.1	98.5	5.83
	Peak 2	46.4	1.5	1.58
	Peak 3	0.00	0.0	0.00

Table S1 showing zeta potential results of CG (bovine gelatin) nanodots

		Mean (mV)	Area (%)	St Dev (mV)
Z-Potential (mV): -20.2	Peak 1	-20.2	100.0	4.38
	Peak 2	0.00	0.0	0.00
	Peak 3	0.00	0.0	0.00

Table S2 showing zeta potential results of CA (algae) nanodots.

The apparent zeta potential of CG (bovine gelatin) nanodots is -30.3 (Fig. S1 A) which indicates good stability and minimum aggregation. The zeta potential of CA (PHM3 algae) nanodots is -20.2 (Fig. S1B). CA (PHM3 algae) nanodots are also negatively charged, however the magnitude is less than CG (bovine gelatin) nanodots which can be the reason of agglomeration as observed in SEM analysis.

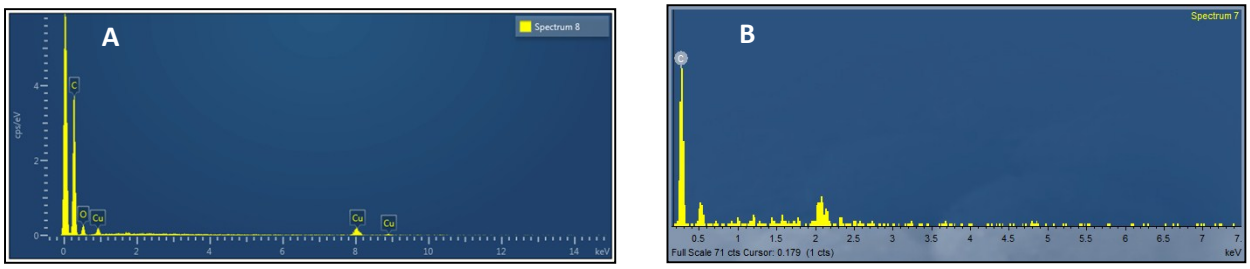

Figure S2 (A) EDX spectrum of CA (PHM3 algae) nanodots) (B) EDX spectrum of CG (bovine gelatin) nanodots

The EDX spectrum of CG (bovine gelatin) nanodots depicts high carbon content with the weight % of 95.06 % as compared to CA (PHM3 algae) nanodots with weight% of 77.91%. However, the weight % of oxygen is more in CA (PHM3 algae) nanodots i.e. 17.52 % as compared to CG (bovine gelatin) nanodots which indicates more surface oxidation in CA (PHM3 algae) nanodots as compared to CG (bovine gelatin) nanodots

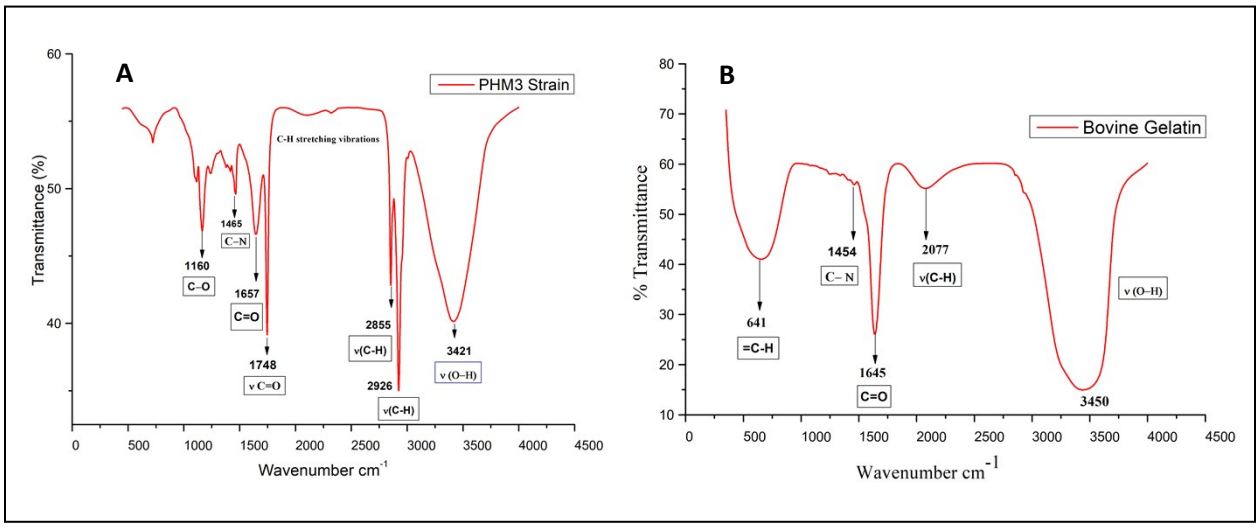

Figure S3 (A) FTIR spectra of PHM3 strain. (B) FTIR spectra of bovine gelatin

In case of algal strain, Fig S3A, the peak at 3421cm^{-1} is due to N-H stretching of protein and O-H stretching of carbohydrates and peaks at 2926cm^{-1} and 2855cm^{-1} are mainly due to CH_2

antisymmetric stretch of methyl groups mainly from lipids [1]. The peak at 1748cm^{-1} is associated with carbonyl groups ν(C=O). Peak at wavenumber 1657cm^{-1} is associated with C=O of amide bond and the peak at wavenumber of 1465cm^{-1} is associated with amine III C-N bond [2]. Similarly, small peaks between 1200cm^{-1} to 726cm^{-1} are associated with the functional groups of carbohydrates. In the case of bovine gelatin Fig S3B, the absorption band at 3450cm^{-1} is associated with ν(O-H) and ν(N-H) stretching vibrations. The absorption band around 2077cm^{-1} indicates stretching vibrations of C-H bonds. The amide I peak was observed at 1645cm^{-1} and is associated with C=O stretching vibration of peptide linkage [3]. A very small peak at 1454cm^{-1} is associated with amide III C-N bonds [2].

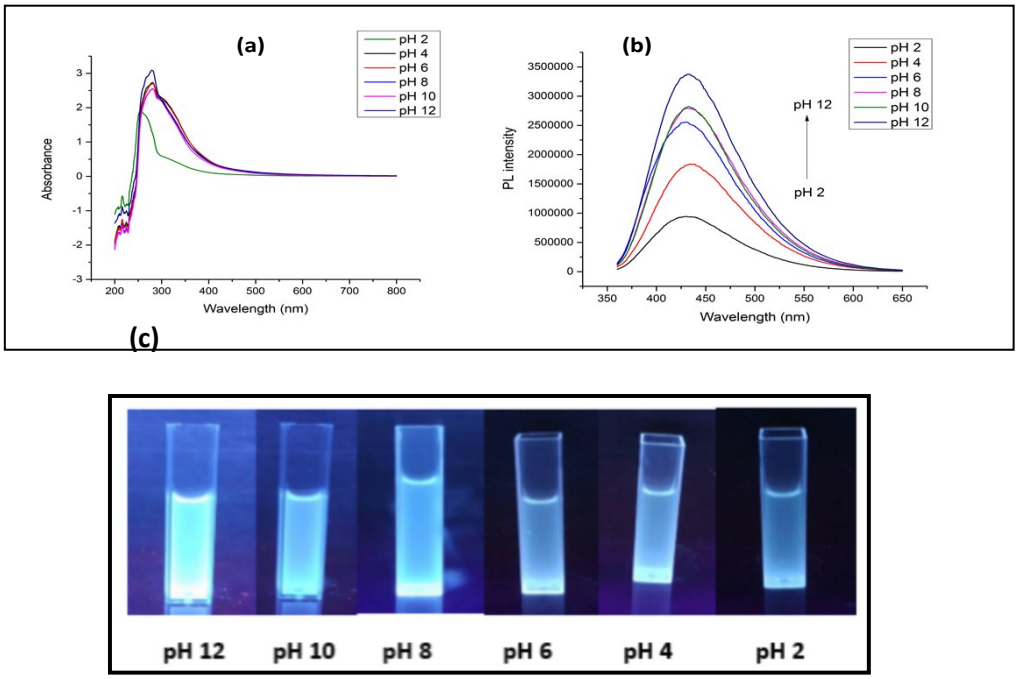

Figure S4 (a) UV-absorption spectra of CG (bovine gelatin) nanodots at different pH (b) PL emission spectra of. CG (bovine gelatin) nanodots at different pH (c) CG (bovine gelatin) nanodots in different pH under UV excitation

Fig. S4a shows the UV spectra of CG (bovine gelatin) nanodots in different pH. The absorption intensity increases as pH increase from acidic to basic. Fig. S3b shows the PL spectra of CG (bovine gelatin) nanodots solution at different pH under a single excitation wavelength of 360nm. At lower pH CG (bovine gelatin) nanodots show low PL intensity but when the pH is increased from 2 to 12 the fluorescence intensity increases with maximum intensity at pH 12. The emission maxima are slightly changed as the pH fluctuates from acidic to basic condition this variation in emission intensity and

emission maxima can be due to ionization of surface groups in different pH solutions. At acidic pH, the electron withdrawing nature of surface groups becomes stronger, because of less probability to form deprotonated type When the conditions are changed to basic from pH 2 to 12, the surface groups become deprotonated thereby reducing the electron withdrawing efficiency, increase in fluorescent intensity with increase in pH can also be observed under 365nm UV excitation in (Fig. S4c). These results support surface state related PL emission rather than size effect, as the parameters of fluorescence emission should be insensitive or weakly sensitive to solvent perturbations.

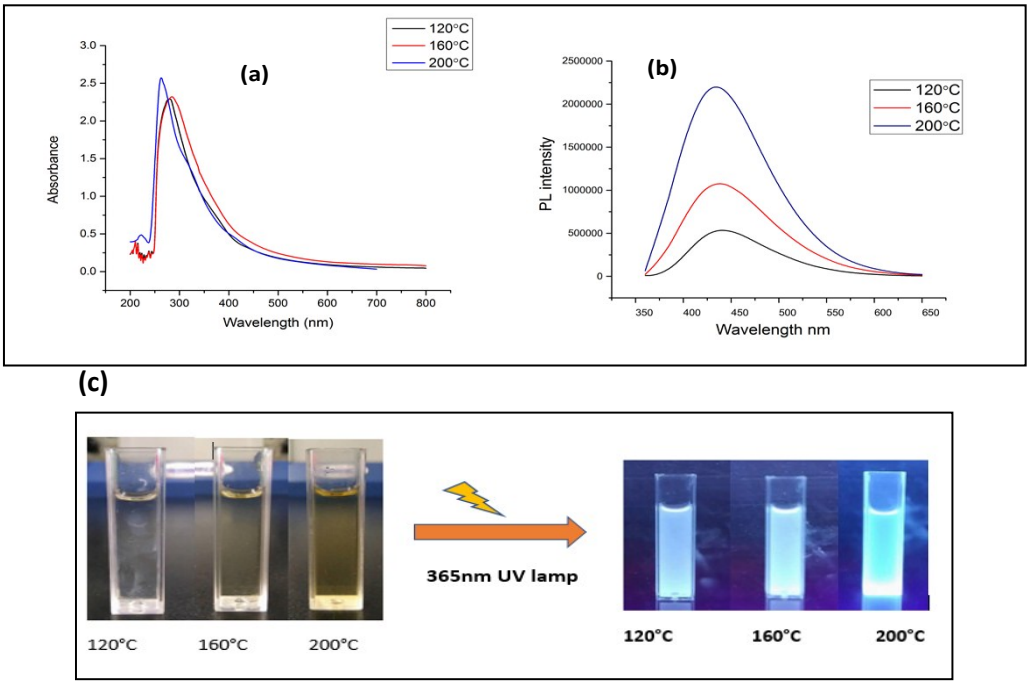

Figure S5 (a) UV-absorption spectra of CG (bovine gelatin) nanodots at different carbonization temperatures (b) PL emission spectra of. CG (bovine gelatin) nanodots at different carbonization (c) solution of CG (bovine gelatin) nanodots prepared at different temperatures in day light and under UV excitation

Fig. S5a shows UV absorption spectra of CG (bovine gelatin) nanodots at three different temperatures. In the absorption spectrum of CG (bovine gelatin) nanodots synthesized at 160°C and 120°C a peak around 300nm is observed whereas absorption spectra of CG (bovine gelatin) nanodots synthesized at 200°C shows a peak at 268nm. A general trend increases in carbonization with increase in reaction temperature is followed here. Fig. S5b shows the PL spectra of CG (bovine gelatin) nanodots at three different carbonization temperatures at an excitation wavelength of 360nm. PL spectra at 200°C shows maximum emission at 434nm with the highest fluorescence intensity. The PL spectra at 160°C shows maximum emission at 438nm with intermediate fluorescence intensity while the PL spectra at 120°C

shows maximum emission at 440nm with lowest fluorescence intensity. As hydrothermal carbonization temperature increases fluorescence intensity also increases with maximum at 200°C which indicates that more of the gelatin protein has been converted in to CG (bovine gelatin) nanodots the increase in fluorescent intensity with increased hydrothermal temperature can also be observed under 365nm UV-excitation lamp (Fig. S5c).

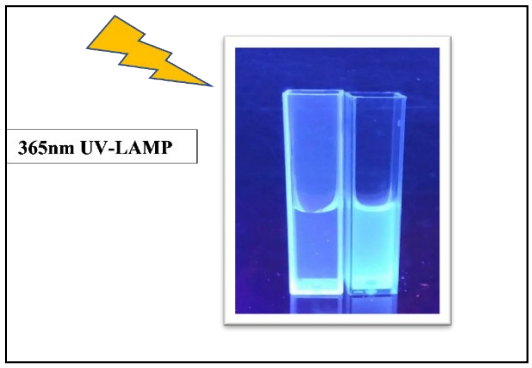

Figure S6 Solution of gelatin(right) and CG (bovine gelatin) nanodots(left) under 365nm UV excitation

FigS6 (right)shows that gelatin itself is non-emissive under UV-light and fluorescence in due to formation of CG (bovine gelatin) nanodots (left).

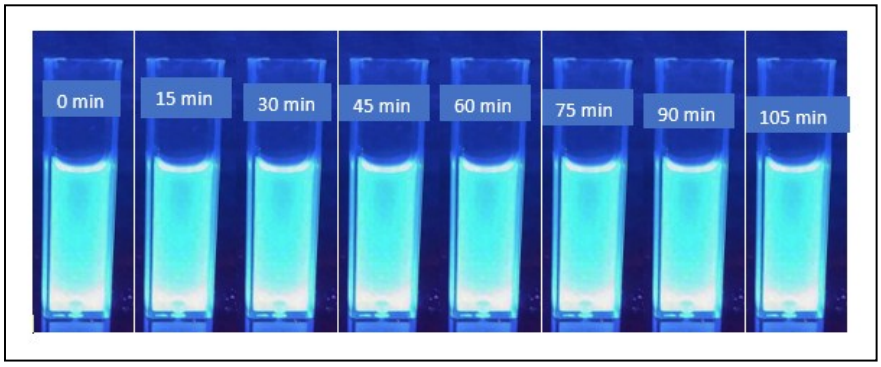

Figure S7 showing photostability of CG (bovine gelatin) nanodots

CG (bovine gelatin) nanodots solution was irradiated by UV light at an excitation wavelength of 365 nm for 105 min at 15 min time intervals. CG (bovine gelatin) nanodots did not show any kind of photobleaching and the fluorescence strength of CG (bovine gelatin) nanodots remained constant even after 105 min of constant UV light excitation, demonstrating the good photostability.

References

1. Bankoti K, Rameshbabu AP, Datta S, Das B, Mitra A, Dhara S. Onion derived carbon nanodots for live cell imaging and accelerated skin wound healing. *J Mater Chem B*. 2017;5(32):6579-6592. doi:10.1039/C7TB00869D.
2. Yang Z, Xu M, Liu Y, et al. Nitrogen-doped, carbon-rich, highly photoluminescent carbon dots from ammonium citrate. *Nanoscale*. 2014;6(3):1890-1895. doi:10.1039/C3NR05380F.
3. Elango J, Zhou Y, Wenhui W, et al. Type II Collagen and Gelatin from Silvertip Shark (Carcharhinus albimarginatus) Cartilage: Isolation, Purification, Physicochemical and Antioxidant Properties. *Mar Drugs*. 2014;12:3852-3873. doi:10.3390/md12073852.